Evaluation of the High-Power Delayed Wave for MIMO-OFDM through Indoor Experiments

[#]Yuki Hirota, Shinobu Nanba, Yoji Kishi
KDDI R&D Laboratories Inc.
2-1-15 Ohara, Fujimino-city, Saitama, 356-8502 Japan, yu-hirota@kddilabs.jp

Abstract

This paper evaluated the influence of the high-power delayed wave on the polarized MIMO-OFDM system which complies with the 3GPP specification through indoor experiments. Authors confirmed that the influence varies greatly by the DFT starting point and relates in the co-polarized received power and the delay time.

Keywords: MIMO-OFDM polarization Delayed wave Experiment

1. Introduction

A MIMO-OFDM combining MIMO (Multiple-Input Multiple-Output) and OFDM (Orthogonal Frequency Division Multiplex) systems is the most promising technology for providing large capacity and high speed transmission in mobile communication systems. The technologies are actually employed in a wide variety of radio access standards such as 3GPP LTE (Third Generation Partnership Project Long Term Evolution) [1]. OFDM is a multi-carrier transmission system to avoid an inter-symbol interference (ISI) which occurs in a large delayed spread environment due to multipath propagation. However, if the delay spread is greater than the guard interval (GI), OFDM transmission quality degrade because an inter-symbol interference (ISI) and inter-carrier interference (ICI) occur and the SINR (Signal to Interference and Noise power Ratio) of the transmit signal degrades. The issue of the OFDM system is discussed in many papers [2-5]. However, these studies assume a low power delayed wave. For further evaluation of the delayed wave issue in OFDM, authors consider the high-power delayed wave to evaluate a MIMO-OFDM system which complies with the 3GPP specification [1]. In this environment the power of the delayed wave is higher than that of the direct wave. For example, a receiver in a building receives a direct wave from the outdoor macro base station and a delayed wave from a repeater installed in the building, respectively. The received power of the direct wave from the base station degrades due to the penetration loss. The received power of the delayed wave from the repeater is higher than that from the base station because the repeater is installed indoors near the receiver. In order to assess the influence of the high-power delayed wave, this paper evaluates the measured data through indoor experiments conducted under the above-mentioned environment. The polarized MIMO, which is effective in the line of sight (LOS) and non LOS (NLOS) environment [6], is evaluated in this paper. The characteristics of a SINR, a noise power and a throughput are evaluated when the ISI and ICI occur due to the delayed wave. The noise power includes both ISI and ICI (P_{I+N}). The next section explains the experimental environment. The result of the evaluation is then presented in Section 3. The final section presents the conclusions.

2. Experimental Environment

The experiments were conducted indoors in LOS environments at 1.5GHz band. Figure 1 shows the layout of the environment in the corridor of KDDI R&D Laboratory, Fujimino-city, Saitama, Japan. The transmitter and the receiver composed of 2x2 polarized MIMO, each of which corresponds to the vertical (V) and horizontal (H) polarization, are contained in one radome, respectively. The transmitter is located at the end of the corridor at a height of 1.6m above the floor. The half-power beam width of the transmitter is 80 degrees. At the other side of the corridor, the receiver is located at a height of 0.7m above the floor. The receiver has omni-directional antenna for the horizontal plane. Authors aimed to analyze the received data including the delayed wave.

Table 1: Specification of the Experiment.

Frequency	1490.9 [MHz]	Band Width	5 [MHz]
Sampling Frequency	10 [MHz]	Delay time	0 – 25 [μsec]
Transmit Power (Max)	0.1 [W] (20 [dBm])	Horizontal and Vertical pattern of Transmit antenna	80 [degree]
Transmit antenna	Directional polarized antenna	Received antenna	Omni directional polarized antenna
Antenna Gains of transmit antenna	7.15 [dBi]	Antenna Gains of received antenna	2 [dBi]
Number of SC	300 (330)	DFT points	667
MCS (Modulation and Coding Scheme)	QPSK 1/2	FEC (Forward Error Coding)	Turbo code
Channel estimation	Non-ideal	Code word	Multiple-code word
Receiver algorithm	MMSE	Bit length	2216

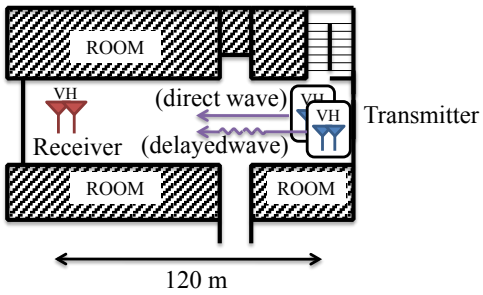

Figure 1: Layout of the experiment.

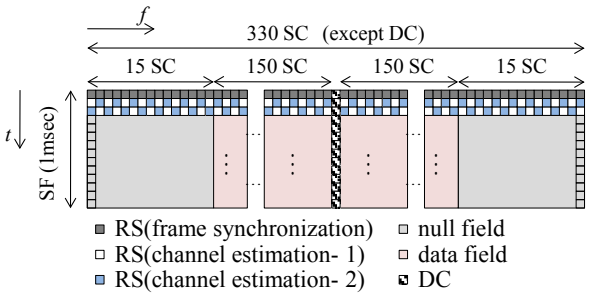

Figure 2: Frame format of the transmit signal.

Another antennas to transmit the delayed wave intentionally besides the antennas to transmit the direct wave in the transmitter are equipped as shown in Fig. 1. The antennas to transmit the direct wave are installed as the base station. The antennas to transmit the delayed wave are installed as the repeater. Moreover, the transmit power of the primary antennas is 10dB lower than that of the secondary antennas because authors assume that the power of the delayed wave is higher than that of the direct wave.

The OFDM signal configuration is shown in Fig. 2. This complies with the 3GPP specifications [1] except for the first three OFDM symbols in the sub-frame (SF) for each antenna. The SF was composed of 14 OFDM symbols and 330 sub-carriers (SC). The first symbol of the SF was used for frame synchronization to determine the DFT starting point. The DFT starting point of the environment is changed according to the direct wave or the delayed wave. Figure 3 shows the image of the DFT processing referring to the direct wave and the delayed wave. The following two symbols were used to estimate the propagation characteristics for each OFDM symbol. The reference symbols (RS) were alternatively inserted in the SCs for both symbols from the two transmit antennas. The remaining OFDM symbols were considered as data fields and null fields. Central SCs are data symbols and outer 15SCs are silent symbols. The duration of the SF and the guard interval is 1msec and 4.7μsec excluding the first OFDM symbol. The guard interval of the first OFDM symbol is 4.9μsec. In the receiver, the received radio signals were recorded as the waveform by IF sampling. The clock timing signals at both sites are provided for synchronization by a GPS 1-PPS (pulse per second) signal at both sites. The other specifications of the experiment systems are provided in Table 1.

3. Evaluation of the Experiment Result

As a first evaluation, the throughput is evaluated for each DFT starting points referring to the direct wave or the delayed wave in Fig. 4 as a function of the delay time. The throughput is calculated using the data field. If the data field of each SF includes the error bits, the SF is discarded.

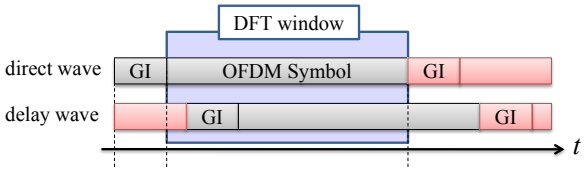

(a) DFT starting point referring to the direct wave

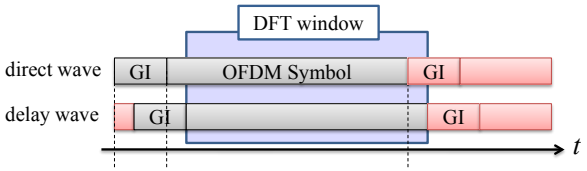

(b) DFT starting point referring to the delayed wave

Figure 3: DFT starting point.

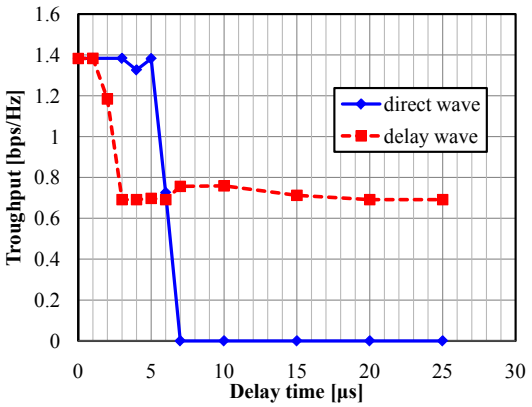

Figure 4: The throughput of each DTF starting point.

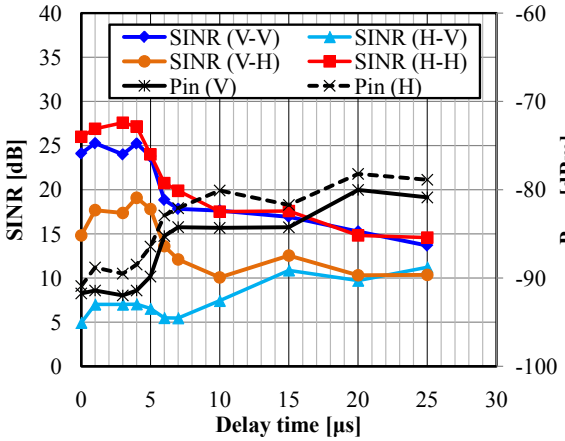

Figure 5: SINR and P_{I+N}. (direct wave)

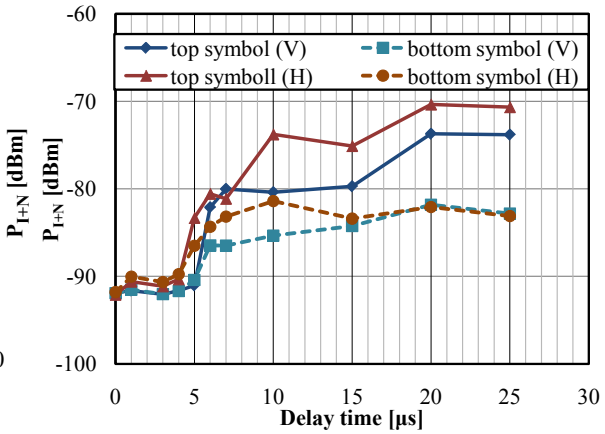

Figure 6: P_{I+N} of the top and bottom symbol.(direct wave)

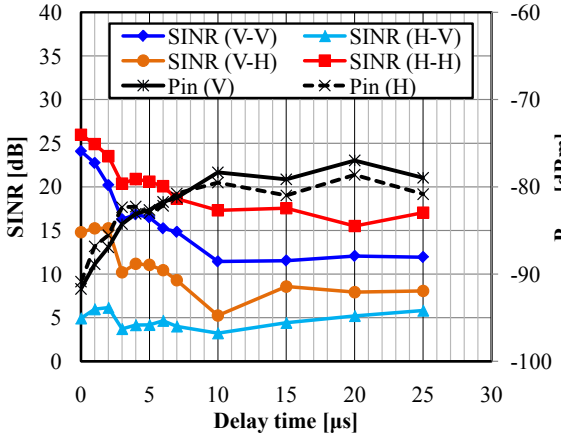

Figure 7: SINR and P_{I+N}.(delayed wave)

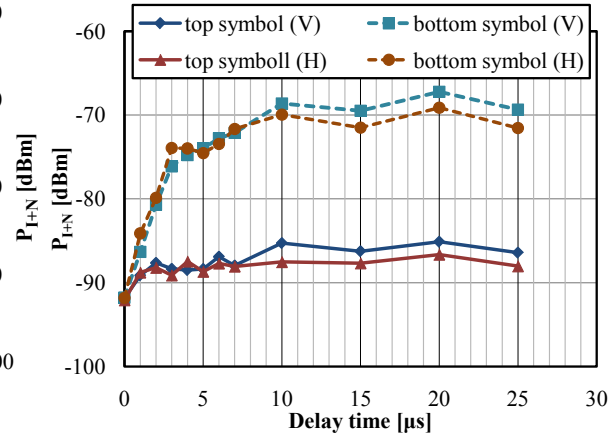

Figure 8: P_{I+N} of the top and bottom symbol. (delayed wave)

The throughput of the former degrades when the delay time exceeds the duration of the GI. In contrast, the throughput of the latter degrades when the delayed wave exists. Moreover, the throughput of the latter does not drop to 0bps/Hz. To analyze the result, SINR and P_{I+N} are evaluated. As the analysis of the former, SINR and P_{I+N} as a function of the delay time are shown in Fig. 5 when the DFT starting point refers to the direct wave. SINR is presented for all combinations of each transmitter and receiver antennas. P_{I+N} is shown for each received antenna. These are described by the polarization of each antenna in the figures. SINR is measured for each SF and averaged for all SFs. P_{I+N} is calculated for null fields. In OFDM processing, the signal is received correctly when the delay spread is less than the duration of the GI [5]. In this case, P_{I+N} increases

and SINR of the co-polarized antenna decreases when the delay time exceeds the GI as expected. Then, in order to analyze the influence of the ISI, the P_{I+N} of the top and bottom symbols in the null fields of each received antenna is shown in Fig. 6. P_{I+N} of the top symbol is larger than that of the bottom symbol when the delay time exceeds the GI. The delayed signal in the 3rd symbol for channel estimation interferes with the direct signal in the top symbol. P_{I+N} of the bottom symbols increases because the bottom symbols in the data field cause ICI. Therefore, SINR and the throughput decrease when the DFT starting point refers to the direct wave and the delay time exceeds the GI. As the analysis of the latter, SINR and P_{I+N} as a function of the delay time are shown in Fig. 7 when the DFT starting point refers to the delayed wave as shown in Fig. 3. P_{I+N} increases and SINR of the co-polarized antenna decreases when the delay time exceeds 1μsec. This is due to the ISI. Figure 8 shows P_{I+N} of the top and bottom symbols in the null fields. P_{I+N} of the bottom symbols becomes much larger than that of the top symbols. It is because the direct signal of the subsequent symbol leaks within the DFT window and interferes in the bottom symbol of the delayed wave as shown in Fig. 3. In contrast, P_{I+N} of the top symbol is sufficiently lower than that of the bottom symbol because the power of the direct wave is lower than the delayed signal. Therefore, Moreover, SINR and the throughput decrease when the DFT starting point refers to the delayed wave and the delay time exceeds the GI. Moreover, when the difference of SINR for the co-polarized antennas in Fig. 7 is compared with that in Fig. 5, the difference of the latter is large though that of the former is small. It is due to the difference of P_{I+N} which occurs by the difference of the co-polarized received power. The received power of the H co-polarization is higher than that of V. Therefore, the ISI by the transmit signal of the H polarization influence the P_{I+N} greatly. The SINR of H-H antenna pair in Fig. 7 is sufficiently high because the influence of the ISI is small in the environment. Thus the throughput by which the DFT point refers to the delayed wave does not drop 0bps/Hz when the delay time is large. From the analysis, it is confirmed that the DFT starting point should be determined by the direct wave when the delayed wave is within the GI in the high-power delayed wave environment. Moreover, authors consider that the throughput is varied by the co-polarized antenna and the delay time. However, further verification in other environment is necessary to evaluate the characteristic of MIMO-OFDM including the polarization.

4. Conclusion

This paper evaluates the MIMO-OFDM system which complied with the 3GPP specification with high-power delayed wave through indoor experiments in the corridor of KDDI R&D Laboratory in Fujimino-city, Saiamata, Japan. As a result, the throughput varies because the influence of the ISI and SINR varies according to the DFT starting point referring to the direct wave or the delayed wave. Therefore, the DFT starting point should be determined by the direct wave when the delayed wave is within the GI in the high-power delayed wave environment because the ISI does not occur. Moreover, authors consider that the throughput is varied by the co-polarized antenna and the delay time.

References

[1] 3GPP TR 25.814, Physical Layer Aspects for Evolved UTRA, v.7.1.0, Sept. 2006.

[2] Y.Sagae, S.Suyama, H.Suzuki, and K.Fukawa, “An OFDM turbo equalizer for scattered pilot signals in multipath environments with delay difference greater than guard interval,” IEEE, VTC2004-Spring, vol.1, pp.425-429, 2004.

[3] Kun.Yan, Hsiao-Chun Wu, Shih Yu Chang, Yiyan Wu, “A novel adaptive prefix interval scheme for MIMO OFDM systems,” IEEE, ISCAS 2009, pp.2798-2801.

[4] Xiantao Sun, Cimini, L.J., Greenstein, L.J., Chan D.S., “ICI/ISI aware beamforming for MIMO-OFDM wireless system,” IEEE, CISS 2009, pp.103-107.

[5] Y.Karasawa, “OFDM Transmission Characteristics where the Delay Profile Exceeds the Guard Interval in Nakagami-Rice Fading Environment,” IEICE Trans. Commun., vol.E91-B, no.10, Oct 2008.

[6] S.Nanba, M.Fushiki, Y.Hirota, and Y.Kishi, “2GHz Band MIMO Propagation Measurement of Dual Polarized Antennas in a Residential Area,” IWCMC 2010, pp.814-818, June. 2010